VULCAN: An Extension of The Smart/Shea Proton Prediction Model

J.Spagnuolo Jr.

U.M. Schwuttke

Cecilia Han

Felipe Hervias

Jet Propulsion Laboratory

California Institute of Technology

Pasadena, California 91109

abstract

The proton prediction **system** (PPS86) developed by Smart and Shea determines the fluxes of solar flare ejected protons in the vicini y of the earth. VULCAN (Visual Utility for the Localization of Corona Accelerated Nuclei) is an extension of PPS86 in that it computes fluxes at arbitrary points of the solar system. Further, VULCAN has interactive graphical components which enhance the user's overall perception of a solar flare's effects upon the solar system while providing him with precise and accurate data of his choice. VULCAN has a predictive capability regarding the times and magn tudes of proton fluxes since the flare related electromagnetic data used to run VULCAN arrives in minutes as opposed t o hours or days for the protons. For JPL operations, advantages associated with this forecasting capability include improved efficiency in solving ground link problems, options for delaying communications between ground stations and spacecraft until peak disturbances have subsided and opportunities for conducting possible science observations. A data base of flare events is maintained and can be used for a

retroactive analysis when it is desired to know if protons from a previous solar flare might have had an effect on certain facets of mission operations.

Introduction

The occurrence of solar flares can cause a variety of difficulties in spacecraft mission operations]. The Magellan mission star tracker problems and certain Galileo bit corruption problems have been attributed to solar flares. Further, solar flares can cause communications failures due to the impact of protons upon the delicate transmitting and receiving equipment aboard spacecraft, Detailed knowledge of the intensity of the proton fluxes over time from a detected flare can provide information to mission personnel that would enable them to minimize the effect of flares on operations. Further, if some aspect of mission operations exhibited unexpected behavior in the past, it would be useful to rule out or demonstrate the possibility that a solar flare might have been the source of the problem. Such a retroactive analysis has already been done with respect to Mars Observer[2] and Topex [3].

Smart and Shea [4][5] and Heckman [6] have devised models which predict the fluxes at earth based upon certain electromagnetic indicators sent out by the flares. The Smart/Shea and Heckman models and their variants [7] yield flux data for earth which is of an order of magnitude of the real flux values.

At JPL, it was desired to determine if any of these existing systems could be extended to predict proton fluxes for points of the solar system other than earth. Further,it was desired to add appropriate graphics which would enhance the user's overall perception of the solar flare's effects upon the solar system while providing him, at any time, with the precise and accurate flux data. The solar flare tool developed at JPL resulting from these specifications is called the Visual Utility for the Localization of Corona Accelerated Nuclei(VULCAN), named after the Roman god of fire. The theoretical basis for VULCAN is the Smart/Shea model, referred to as PPS86. Smart and Shea described how to extend their model to

the inner heliosphere and were readily available for discussions on the scientific as well as practical aspects of their work. These reasons together with the long documentation and implementation history characterizing PPS86 made it a good choice for the basis of VULCAN.

VULCAN relies on 1-8 A° X-ray data from the National Oceanographic anti Atmospheric Administration for indication of solar flare activity. The peak flux, the time of detection and the latitude anti longitude associated with the flare are also sent. Required planetary data is provided by the SPICE[1] [8] system from the Navigation Systems Section of The Jet Propulsion Laboratory.

Advantages of using VULCAN include improved efficiency in solving ground link and instrumentation failure problems, specific options r-elating to the delay of communications between ground stations until peak disturbances have subsided, and possible opportunities for conducting science observations. It should be mentioned that the consensus of the scientific community is that the underlying theory used in the determination of proton fluxes is valid if the point of prediction "1s near the plane containing the solar equator. For points away from the solar equator, breakdown of the propagation theory may occur. VULCAN has the capability of incorporating arbitrary trajectories into its graphics and computational modules to derive a prediction of fluxes at. points away from the solar equator, thus enabling experimentation with the program to determine the 1 imits of the theory.

Flare Angle Determination

Background

In [9] and [10], Smart and Shea prescribe how to extend their model to various points in the inner heliosphere near the plane of the solar equator. In addition to their specifications, a procedure which we refer to as the flare angle extrapolation algorithm had to be created to properly compute the fluxes at these points. In this section we will discuss the algorithm and its associated computations.

1.The SPICE sysytem provides ephemeris data and associated software which accurately computes the positions of the sun and planets over specified periods of time.

Data used to run VULCAN is sent from the Space Environment Laboratory of the National Oceanic and Atmospheric Administration in Boulder Colorado. Aside from parameters relating to the time of the flare and its associated X-ray data, the latitude and longitude of the flare with respect to the earth[2] are sent. The purpose of the flare extrapolation algorithm is to use these angles to determine the location of the flare with respect to an arbitrary point in space at which we wish to compute the fluxes.

Geometry

In order to describe the flare angle extrapolation algorithm, certain geometrical aspects of the problem together with appropriate definitions will first be presented.

We define the ε-sun plane to be the plane containing the center of the earth and the north and south poles of the sun and the τ-sun plane to be the plane containing the center of an arbitrary point in space, τ, and the north and south poles of the sun. We further define the ε-point to be the point contained n the intersection of the ε-sun plane and the solar equator which is closest to the earth. Similarly, we define the τ-point to be the point in the intersection of the τ-sun plane and the solar equator which is closest to τ. A side view of this perspective is illustrated in figure 1(a). Here, the 4 stars represent the north and south poles of the sun and the center of the earth and target. The dashed curved lines represent the intersections of each of the planes with the sun's surface. As shown, $\phi_{\varepsilon,\tau}$ is the angle between the ε-point and the τ-point along the solar equator. It is this angle that we define as the angle between the earth and τ. Figure 1(b) represents a top view of this orientation. Since the familiar generalized form of the pythagorean theorem is used to derive $\cos(\phi_{e,\tau})$, we have $0 \le \phi_{e,\tau} \le \pi$. An appropriate sign will be given to the angle $\phi_{e,\tau}$ based upon considerations presented in the following discussion.

2.The meaning of the phrase 'latitude and longitude with respect to x' will be moe precisely expressed in the following discussion.
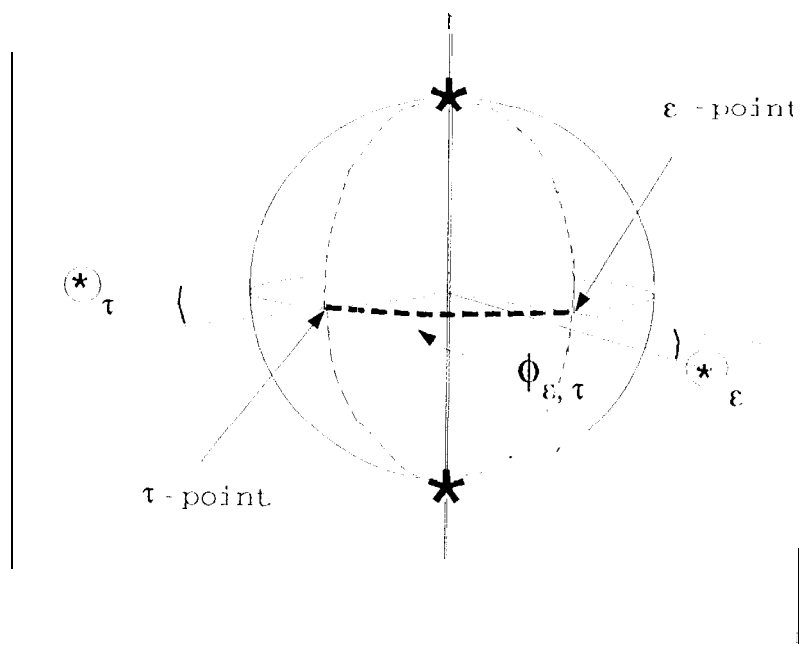
(a) side perspective of ε-sun plane and τ sun plane
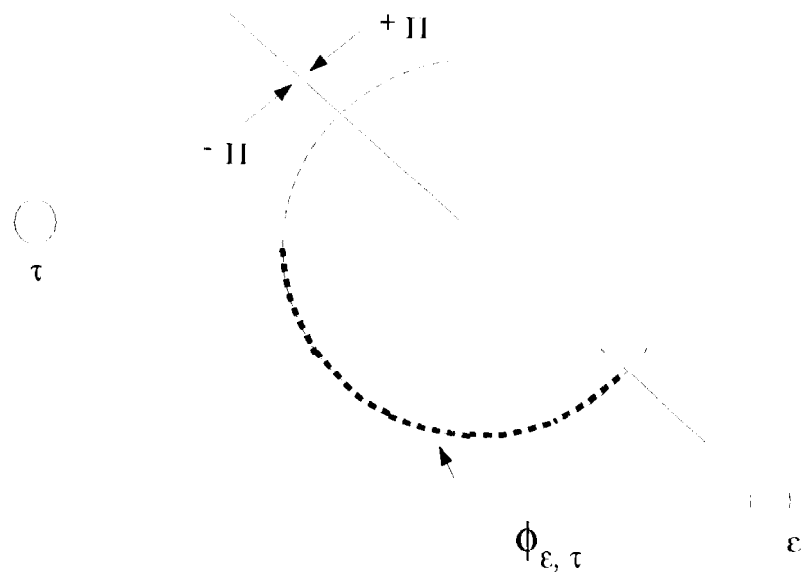
(b) top perspective of ε – sun plane and τ sun plane

Figure 1

Target and earth planes side and top views

As mentioned earlier, the latitude and longitude of the flare are computed and sent to VULCAN by NOAA at Boulder Colorado. The latitude of the flare is measured from $[0$ to $\pi/2]$ and from $[0$ to $-\pi/2]$ going from the solar equator to North Pole and South Pole respectively. As labeled in Figure 1(b) positive longitude is measured counter-clockwise (from the vantage point of the North pole on the solar equator) from $[0$ to $\pi]$ where 0 is the ϵ-point. Negative longitude is measured clockwise from $[0$ to $-\pi)$. It should be emphasized that the longitude of a flare with respect to an arbitrary point τ in space is subject to the same interval conventions as mentioned above except that the flare longitude is measured in relation to the τ-point. The theory underlying VULCAN is such that if it is desired to compute the flux at a point in space, then the latitude and longitude of the flare with respect to the point (measured as described above) must be used in the computation. If L is a line drawn from sun center to the center of the point in space, and If $\phi_{L,p}$ is the angle between this line and the solar equator, and λ_p tis the latitude of the flare on the sun, then the latitude of the flare with respect to the point is easily given by $\lambda_p - \phi_{L,p}$. However, due to the fact that the longitude of the flare is given with respect to the ϵ-point (and not with respect to a fixed location on the sun such as the solar equator for latitude), the longitude with respect to the earth as sent by Boulder does have to be adjusted in a more coomplicated fashion to compute flux for points other than at earth. The purpose of the flare angle extrapolation algorithm is to compute this adjusted longitude g ven the longitude of the flare as sent by Boulder . In order to derive the proper longitude to compute t he f lux at a point τ, we must use the flare longitude with respect to earth and the longitudinal angle $\phi_{\epsilon,\tau}$ which was as shown in Figure 1(b).

A demonstration of what is involved in this computation involves a consultation of Figure 2. Here, the angle ϕ_F represents the longitude of the flare with respect to the earth. The quantities $\phi_{\epsilon,\tau_{p1}}$ and $\phi_{\epsilon,\tau_{p2}}$ are the angles between the earth and the points at positions 1 and 2 respectively. The positions of the
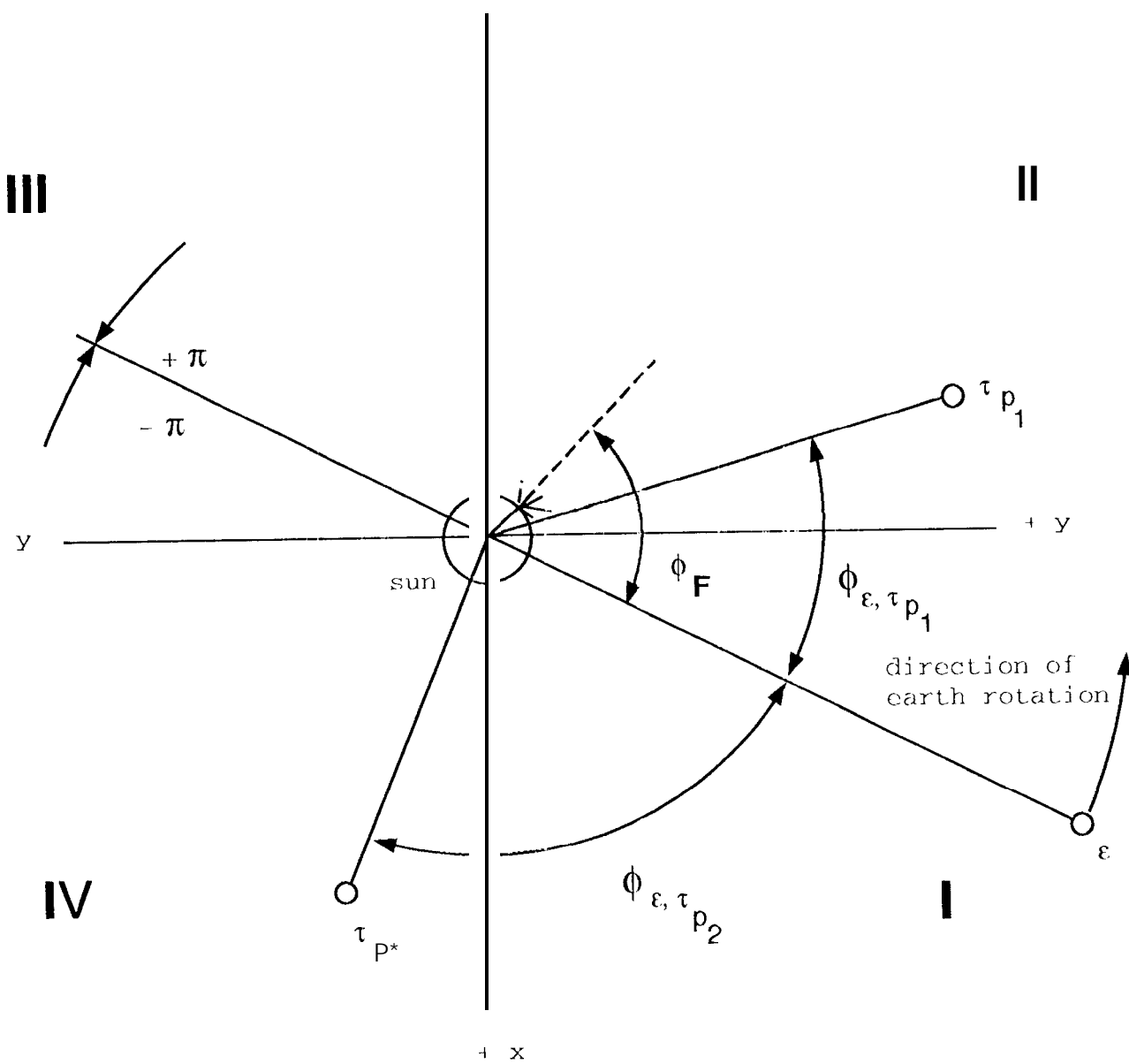
Figure 2

orbital perspective of target anti earth

planets are computed with respect to an x-y-z coordinate system where the x - y plane rests in the plane of the solar equator. The quadrants are numbered as indicated. In general, to determine the longitude of a flare with respect to a point in space, the algorithm first computes the magnitude of the angle between the earth and the point in space as defined earlier and then, by examining the flare angle, the flare extrapolation algorithm does a case by case treatment based upon the quadrants that the planets are in[3] (which is based on the ε-point and the τ-point). Using these cases the program determines whether or not to add plus or minus the angle between the earth and τ to the already known flare angle for the earth to obtain the angle between τ and the flare. For example, if the earth is in quadrant I and if τ is in quadrant II as shown in Figure 2, the angle between the target at position 1, τ_{P_1}, and the flare is $\phi_F - \phi_{\varepsilon,\tau_{p_1}}$. Further, if the earth is in quadrant 1 and τ is in quadrant 2 then the angle between the flare and τ at position 2 is $\phi_F + \phi_{\varepsilon,\tau_{p_2}}$. In cases where the angle falls out of the intervals $[0, \pi)$ and $[0, -\pi]$ mentioned earlier, the program will properly adjust it, thus yielding the longitude of the flare with respect to τ. This adjustment procedure is further discussed below.

In many cases, knowing which quadrants the earth and target are in is not sufficient for determining $\phi_{\varepsilon,\tau 0}$. For example, if the earth and target are in the same quadrants or are in opposite quadrants (1 and III or II and IV) it is not clear whether to add $\phi_{\varepsilon,\tau}$ to or subtract it from $\phi_{e,t}$ to determine the longitude of the flare with respect to the point τ. In these cases, the arctan function is used to determine the relative positions of flare anti target. For example, in Figure 3, a target in quadrant III could be in positions 3 or 4. In position 3, the angle between the flare and τ is $\phi_F - \phi_{\varepsilon,\tau_3}$. However, if τ is at position 4, the angle between the target and the flare is $\phi_F + \phi_{\varepsilon,\tau_{p4}}$[4]. If a target is in the

3. The quadrants are based upon the ε-point and the τ-point as discussed earlier.

4. Note that (for this example according to the diagram) this angle falls outside of the prescribed longitudinal intervals of $[0,\pi], [0,-\pi)$. When this happens, the algorithm adds -2π to its value so that it does fall in the prescribed intervals.
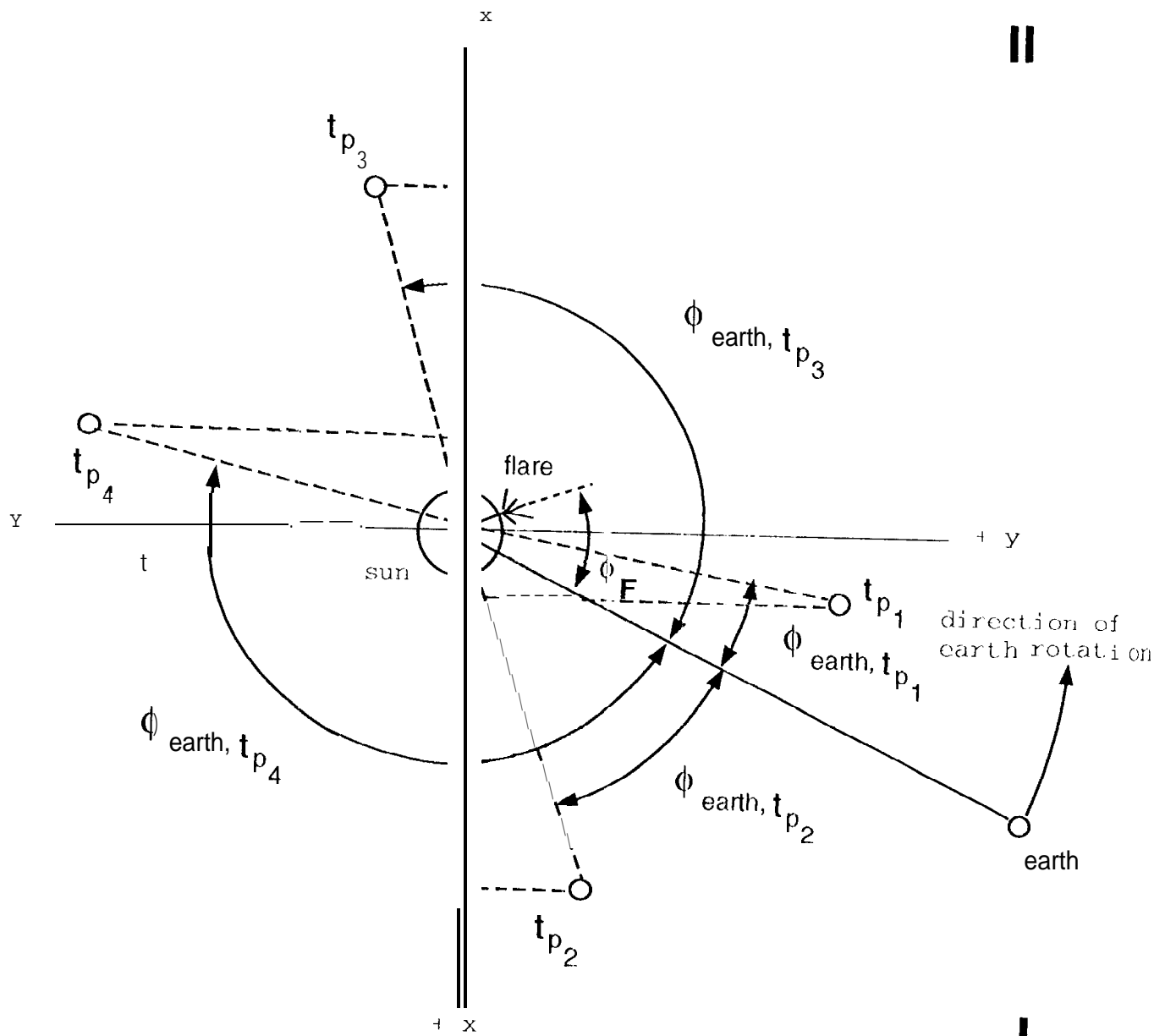
Figure 3

Positions requiring arctan treatment

same quadrant as the earth, ambiguities arise as well. In position 1, the angle between the flare and τ is $\phi_F - \phi_{\mathcal{E},\tau_{p1}}$ whereas in position 2 the angle is $\phi_F + \phi_{\mathcal{E},\tau_{p2}}$. These ambiguities are resolved by use of the arctan function. For example, it can be determined, that in quadrant I $\arctan(y_{\tau1}/x_{\tau1}) > \arctan(y_{\mathcal{E}}/x_{\mathcal{E}})$. We can use this information to conclude that $\phi_{\mathcal{E},\tau_{p1}}$ can be subtracted from ϕ_F to obtain the correct angular distance between τ and the flare when τ is in position 1. Further, using the fact that $\arctan(y_{\tau2}/x_{\tau2}) < \arctan(y_{\mathcal{E}}/x_{\mathcal{E}})$, the algorithm adds the angle $\phi_{\mathcal{E},\tau_{p2}}$ to ϕ_F when τ is in position 2 to determine the angle between the flare and τ_{p2}. Using similar reasoning for the third quadrant, the fact that $\arctan(y_{\tau3}/x_{\tau3}) < \arctan(y_{\mathcal{E}}/x_{\mathcal{E}})$ can be used to determine that the angle between the target at position 3 and the flare is $\phi_F - \phi_{\mathcal{E},\tau_{p3}}$. Also, sine-c $\arctan(y_{\tau4}/x_{\tau4}) > \arctan(y_{\mathcal{E}}/x_{\mathcal{E}})$, the angle between the flare and τ_4 is $\phi_F - \phi_{\mathcal{E},\tau_{p4}}$. The computations in the algorithm take into account not only the signs of all angles but their relative magnitudes as well. We note that the geometrical relations displayed here were only examples used to illustrate some of what had to be considered in order to determine the angle between τ and F given an initial configuration of $\mathcal{E}$, τ and F.

Analysis

In the last section, we gave an overall view of the spatial orientation between points (representing planets, spacecraft etc.) which were determined by certain planes intersecting the solar equator. In this section, we determine the coordinates of an arbitrary 'x'-point given the coordinates of an arbitrary point x . From this, we can then find a general form for the distance between the $\mathcal{E}$-point and the sun center, a τ-point and the sun's center and the distance between the $\mathcal{E}$-point and the τ-point. This enables us to determine the angle, $\phi_{\mathcal{E},\tau}$, between the earth and τ using the generalized pythagorean theorem. We assume that the Cartesian plane in which all computations are done has as its origin the center of the sun

with $+z$ and $-z$ axis passing through the North and south poles of the sun.

Given that τ is an arbitrary point in space, we first determine the equation of the τ-sun plane. The general equation of a plane given by

$$A(x-x_0)+B(y-y_0)+C(z-z_0)=0 \qquad (1)$$

can be reduced, in the case of the τ-sun plane, to

$$Ax+By+Cz=0 \qquad (2)$$

due to the fact that it does, by definition, contain the origin. Since the north pole (as well as the south pole) is also in the plane, it is true that

$$Cz_N = 0 \implies C = 0 \qquad (3)$$

where the coordinates of the North Pole are given by $(0,0,Z_N)$. Since the point $(x_p, y_p, 0)$ is the projection of the center of τ in the x-y Cartesian plane, it satisfies the equation and we have

$$Ax_p + By_p = 0 \qquad (4)$$

Dividing through by A and renaming B/A to K , we have that

$$x_p + Ky_p = 0 \implies K = \frac{-x_p}{y_p} \qquad (5)$$

implying that the general equation of the τ-sun plane is

$$x - \frac{x_p}{y_p} y = 0 \qquad (6)$$

To find the exact coordinates of the τ-point it is first determined that

$$x^2 + y^2 = r_\odot^2 \qquad (7)$$

which implies that

$$x = \left(\frac{x_p}{y_p}\right) y = \left(\frac{x_p}{y_p}\right)\left(\pm \sqrt{r_\odot^2 - x^2}\right) \tag{8}$$

Rearranging terms gives

$$x^2 = \left(\frac{x_l}{y_l}\right)^2 r_\odot^2 - \left(\frac{x_l}{y_l}\right)^2 x^2 \tag{9}$$

and

$$x^2\left(1 + \left(\frac{x_p}{y_p}\right)^2\right) = \left(\frac{x_p}{y_p}\right)^2 r_\odot^2 \tag{10}$$

Thus , the possible coordinates for the t-point are

$$x = \pm \frac{r_\odot \left(\frac{x_l}{y_l}\right)}{\sqrt{1 + \left(\frac{x_l}{y_l}\right)^2}} \tag{11}$$

and

$$y = \pm \frac{r_\odot}{\sqrt{1 + \left(\frac{x_l}{y_l}\right)^2}} \tag{12}$$

The plus and minus values are due to the fact that the t-plane intersects the solar equator in 2 places[5]. We compute the distance from $(x_p, y_p, 0)$ to each set of coordinates $(x+,y+,0)$ and $(x-,y-,0)$ where the former denotes the positive roots of (11) and (12) and the latter gives the negative roots. We then choose the coordi-

5. Note that there are only two pairs of coordinates (as opposed to 4) because from (6) the positive root is used for y <> the positive root is used for x.

nates which represent the point which is closer to $(x_p, y_p, 0)$ since the distance from

⟨ ... ⟩ is the distance from $(x_p, y_p, 0)$ to the point

directly opposite the τ-point on the solar equator. In mathematical terms, if we

define

$$d_i = \sqrt{\left(x_p + (-1)^i \sqrt{\frac{r_0^2}{(\frac{x_p}{y_p})^2 + 1}} \left(\frac{x_p}{y_p}\right)\right)^2 + \left(y_p + (-1)^i \sqrt{\frac{r_0^2}{(\frac{x_p}{y_p})^2 + 1}}\right)^2} \qquad (13)$$

then

$$\tau - \text{point} = \begin{cases} (x+, y+) & \text{if } d_0 = \min\{d_0, d_1\} \\ (x-, y-) & \text{if } d_1 = \min\{d_0, d_1\} \end{cases} \qquad (14) \ .$$

Graphics

Archimedean Spiral

For points in the, inner heliosphere near the plane of the solar equator, present

models of solar particle transport assume that the protons travel along a pathway

in the form of an Archimedean or Parker Spiral [11] given by

$$\rho = a\,\theta \qquad 0 \le \theta \le \xi \qquad (15)$$

where ξ (which will be more fully discussed below) is related to the Archimedean

angle Φ_A with respect to that point[6] and a is the distance from the sum to the point

in question divided by ξ. In what follows, we discuss how to graphically construct

the Archimedean spiral. For purposes of exposition, we will assume that t is in

6.The Archimedean angle with respect to a point τ is defined as the angular distance that the sun rotates in the time it takes for a particle to go from the sun to τ assuming it leaves the sun in a radial path. This is also expressed by the formula $\Phi_A = \omega\,r/V$ where ω is the angular rotation rate of the sun, r is the distance from the sun to the point and V is the speed of the particle.

the plane of the solar equator.[7] The graph of the above function has the approximate form as shown in Figure 4(a). The astronomical interpretation of this graph is realized by embedding it in the sun-τ spatiality as shown in Figure 4(b). The correspondence of the labels α, β, η, and κ in diagrams (a) and (b) indicate the fact that the spiral shape in (a) was flipped and rotated to obtain the orientation as displayed in (b). The view in Figure 1(b)is from a Northerly perspective. The line indicated by d(sun,t) is the length of the line connecting the sun to the point τ. The angle that the graph makes with the line connecting the sun with t is interpreted as being Φ_A. The graphical creation of the shape of the Archimedean spiral thus has two requirements:

(1) It must be of the form as given by (15)

and

(2) It must be such that when one end is placed at sun's center and the other at$τ_{t}$, as shown in Figure 4(b), its intersection with the solar equator is at longitude Φ_A , the given calculated Archimedean angle for the point τ.Both (1) and (2) above require the determination of he angle ξ. To this end, we note that, based on both diagrams in Figure 4,
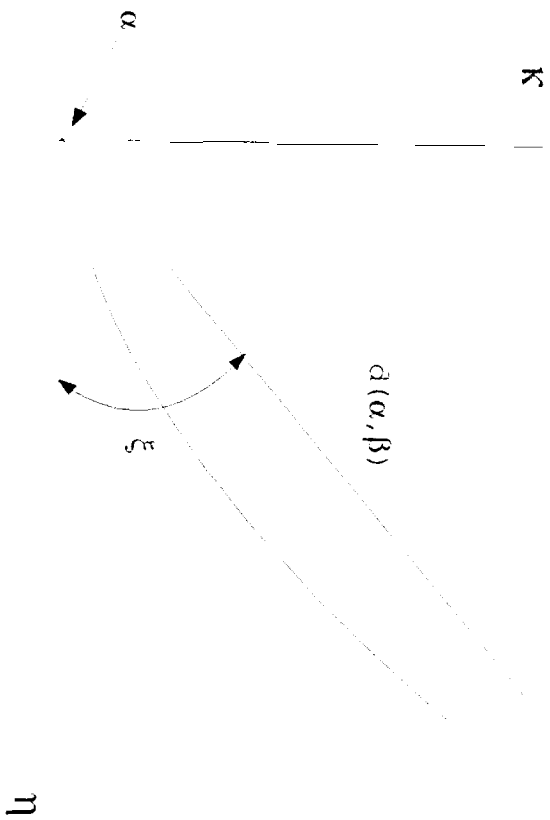
$$r_{\cdot} = a(\xi - \Phi_A) \qquad (16)$$
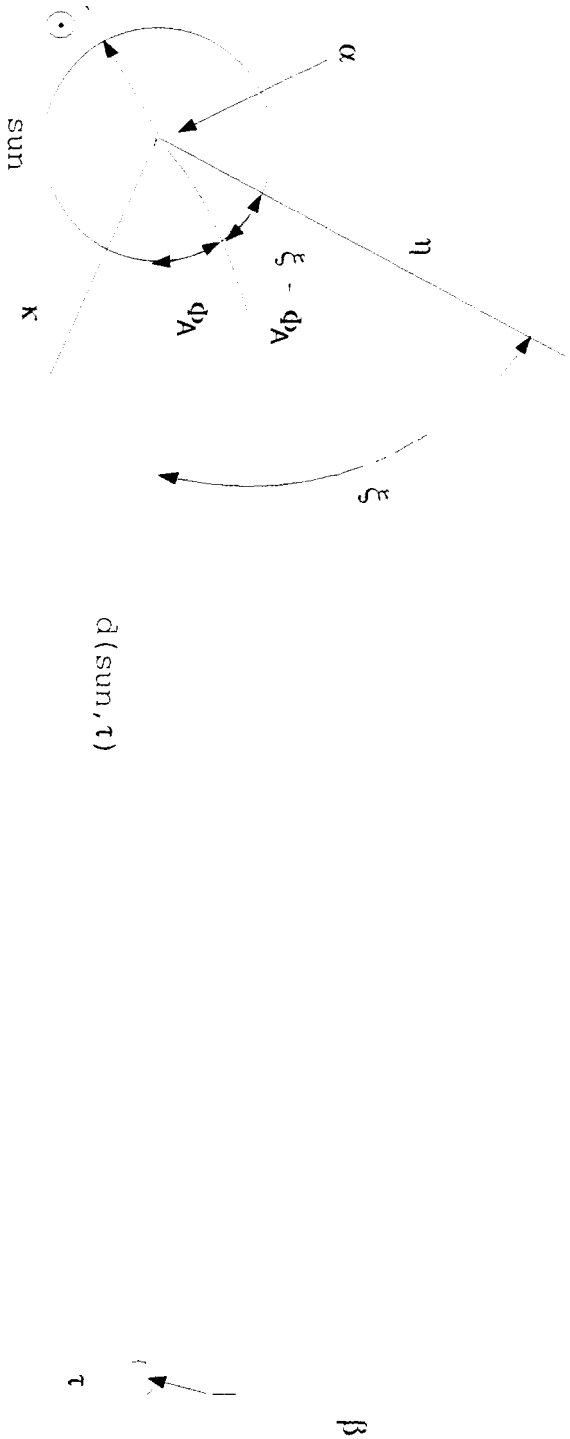
and

$$d(\odot, \tau) = a\xi \qquad (17)$$

Eliminating a gives

$$\frac{r_{\omega}}{\xi - \Phi_A} = \frac{d(\odot, \tau)}{\xi} \qquad (18)$$

7.If τ is not in the plane of the solar equator, we can visualize rotating it into the solar equator and going through the spiral construction reasoning identical to that which is embedded in the following discussion.The computationally visualized spiral for τ in its original position is then obtained by returning the rotated point τ back to its original position with the constructed spiral attached where its shape and orientation with respect to the solar equator in which it was constructed remain unchanged.

(a) Graph of $\rho = d(\alpha,\beta) \cdot 0$ for $0 \leq 0 \leq \xi$.

(b) Above ρ curve embedded in sun-τ relationship

Figure 4

Archimedean Spira Analysis

Cross mu) t j plyi rrg and expandi ng gives:

$$f\{? \ ' ., \ - \ d((\odot),\tau)) = \Phi_A \, d((\odot),\tau) \qquad (19)$$

resulting in

$$\xi = \frac{\Phi_A}{1 - \frac{r_{\odot}}{d(\odot,\tau)}} \qquad (20).$$

The magnitude of the difference of the two angles is

$$\xi - \Phi_A = \frac{\Phi_A}{\frac{d(\odot,\tau)}{r_{\odot}} - 1} \qquad (21)$$

For computations where real astronomical parameters are used,

$$\frac{d((\odot),\tau)}{r} \gg () \Rightarrow \xi \approx \Phi_A \qquad (22).$$

However, in cases for graphical presentation, the relational magnitudes of distance as related to planet size are considerably different from those used in realistic computations characterizing solar physics. To facilitate display, the ratio of the distance between the sun and τ to the radius of the sun may not be that large, implying that the difference between Φ_A and ξ is not that small thus justifying the above treatment.

Visual   configurations

Background

There are essentially two ways that VULCAN has of expressing solar flare data

to the user. The first is intuitive. The second is analytical. Upon reception of solar flare data, The former gives an immediate overall view of the solar flux conditions at various points of the inner heliosphere while the latter allows the user to obtain more precise flux related data at a point of his choosing. These two modes of computational perception complement one another in the sense that the point which the user chooses to analyze using the perspective afforded by the second mode is generally influenced by the overall view of the flux intensities displayed the first mode.

Solar System Graphics

Figure 5 gives the windows comprising the intuitive treatment of the solar system. The leftmost window has a listing of the received flare events from Boulder. Reading from left to right yields the number[8], day and UT (Greenwhich Mean Time) time of the event. The two coordinates at the end of each line are the latitude and longitude of the flare with respect to the ʄ-point. The user chooses the flare event of interest by double clicking on the event. This will be more fully discussed in the following paragraphs. Note that the most recent events occur towards the bottom of the list. For the display in this figure, event #116 was chosen.

If he desires, the user can enter his own flare event by choosing the button Enter Flare Event. When this is done, the screen appearing in the lower right hand corner appears with entries for the various flare parameters needed to run the program. A subset of the parameters to be entered by the user are shown in the diagram. When the user has filled in the desired values and clicks on the button-named Add Event, the flare event is added into the electronic record of flare events in the left-hand window.

Underneath the record of events is a listing of planets and spacecraft. The user can determine whether or not the planet or spacecraft and its trajectory is shown (in the screen to the upper right) by clicking its corresponding box on(non-
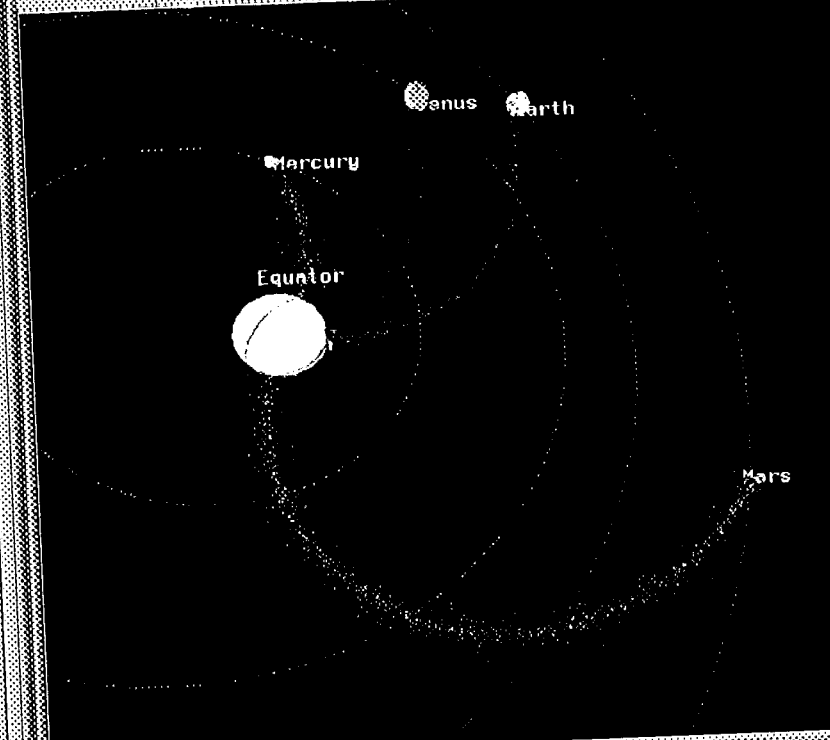
8. For user reference only.

Flare Events

[88] 94/01/27 03:41 (Lat: N08, Lon: N60)
[89] 94/01/81 04:00 (Lat: N11, Lon: N65)
[90] 94/01/28 15:40 (Lat: N08, Lon: N85)
[91] 94/02/20 01:04 (Lat: N09, Lon: N02)
[92] 94/02/24 03:24 (Lat: N12, Lon: N10)
[93] 94/06/14 00:06 (Lat: N01, Lon: N46)
[94] 94/06/01 06:31 (Lat: N13, Lon: N04)
[95] 94/06/24 10:22 (Lat: N13, Lon: E30)
[96] 94/06/30 02:42 (Lat: N13, Lon: E38)
[97] 94/06/30 07:54 (Lat: N10, Lon: E36)
[98] 94/06/30 08:55 (Lat: N18, Lon: E37)
[99] 94/06/30 21:13 (Lat: N18, Lon: E27)
[100] 94/07/05 21:04 (Lat: N10, Lon: N34)
[101] 94/07/06 16:43 (Lat: N09, Lon: E23)
[102] 94/07/06 23:30 (Lat: N08, Lon: E25)
[103] 94/01/07 09:01 (Lat: N13, Lon: E19)
[104] 94/01/07 11:34 (Lat: N11, Lon: E14)
[105] 94/01/07 15:21 (Lat: N10, Lon: E10)
[106] 94/01/07 19:36 (Lat: N10, Lon: E11)
[107] 94/07/12 09:11 (Lat: N12, Lon: N52)
[108] 94/07/13 16:47 (Lat: N12, Lon: N60)
[109] 94/07/18 11:45 (Lat: N10, Lon: E72)
[110] 94/08/14 17:29 (Lat: N12, Lon: N08)
[111] 94/08/15 12:38 (Lat: N18, Lon: N10)
[112] 94/08/17 00:48 (Lat: N16, Lon: N15)
[113] 94/08/18 02:58 (Lat: N08, Lon: N63)
[114] 94/08/19 07:00 (Lat: N09, Lon: N61)
[115] 94/08/20 07:52 (Lat: N06, Lon: E82)
[116] 94/08/30 10:44 (Lat: N08, Lon: E83)
[117] 94/09/11 04:41 (Lat: N11, Lon: N73)
[118] 94/10/08 06:31 (Lat: N11, Lon: N46)
[119] 94/10/01 16:30 (Lat: N11, Lon: N54)
[120] 94/10/13 20:43 (Lat: N12, Lon: N24)
[121] 94/10/28 09:47 (Lat: N06, Lon: N11)

Enter Flare Event

Planets

☐ Mercury   ☐ Venus   ☐ Earth   ■ Mars   ■ Jupiter

■ Saturn   ■ Uranus   ■ Neptune   ■ Pluto

Spacecrafts

■ Ulysses   ■ Galileo

Show Plots

Exit   Graphics on View   Error Ranges   Hide

File Demos Grids Options

Translation   Rotation   Hour   36

Day   302

Year   1994

☐ Insignificant
☐ Significant Threshold =   0.2
☐ Serious Threshold   0.6
■ Critical Threshold =   0.66

Venus   Earth

Mercury

Equator

Mars

Enter In Solar Flare Event

Date of Flare (YY/MM/DD)

Time of Flare (HH:MM)

Latitude (-90 to 90)

Longitude (-180 to 180)

Cancel   Add Event   Hide

Fig. 5

white color) or off (white). The show plots box allows interface to the analytical portion of the graphics, which will be discussed later. The upper right hand corner of the screen is the solar system display window. It allows for the visualization of the solar system from various angles of the user's choosing. In the uppermost panel of this window, the File menu allows the user to reset the visual display to that of the most recent event. The Demos menu has 2 items. The first is Demo Mode. When this is chosen, the solar system display automatically rotates with default planetary settings to show the user the heliosphere from all angles and distances. The second entry of the Demos menu is Show Formation of Spiral. When this is chosen, the Demo Mode menu entry is automatically activated together with an overlying display showing the dispersion of solar particles into the solar system as a result of the rotation of the sun and the solar wind. The Grid menu has six entries: Mercury, Venus, Earth, Mars, Solar Equator and Intersection. If a planet is selected, then a grid containing the orbit if that planet is displayed. For the Solar Equator entry, a grid containing the plane of the solar equator is displayed. Finally, Intersection represents the colored earth-sun plane as described earlier in the paper and is displayed for any relative position between the earth and sun. The Options menu has the entries Show Sun's Movement, Show Archimedean Angle, Show Spiral. Show Sun's Movement shows the rotation of the sun on its axis. For any planet τ, Show Archimedean Angle displays a line emanating from the sun's center through the solar equator where the angle between this line and the τ-point is the Archimedean angle with respect to τ. Show Spiral gives the Archimedean spiral emanating from sun center to the various planets and spacecraft in the display. The Translation and Rotation of the solar system view with respect to the various axes is accomplished in the indicated windows. By using the sliders indicated by hour day and year, the user can display the relative positions of the planets and indicated by hour day and year, the user can display the relative positions of the planets and spacecraft at various points in time. When a flare event is selected, the planets and spacecraft appearing in the solar system view automatically assume their proper juxtaposition corresponding to the time of that event. The next window has slots representing various user defined flux thresholds in ascending order of
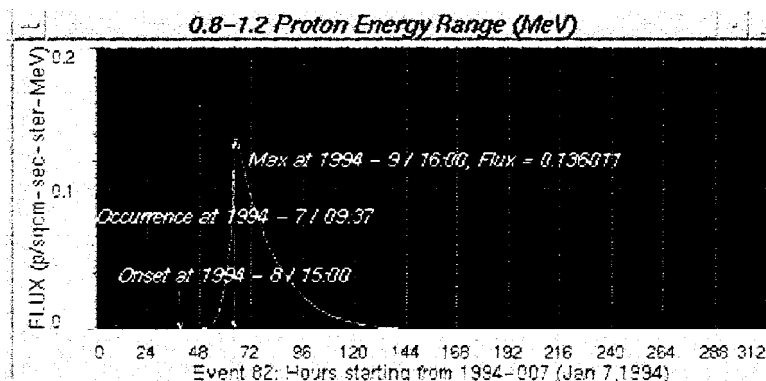
seriousness. When a user selects a flare event from the flare events window, then for each point selected in the planets and spacecraft panels, a flux graph is generated yielding the proton flux for the 300 hours after the time of the selected flare event. Given any chosen planet or spacecraft, τ, the color of the spiral connecting the sun to τ is the color corresponding to the maximum valued user selected threshold which the maximum value of the flux graph[9] of τ exceeds. The threshold values as shown were chosen for purposes of color illustration regarding the spirals in the solar system panel display. In the solar system display panel, the perspective shown is from the south pole of the sun. This is to optimize the visibility of the flare which occurs in the southern hemisphere of the sun. The view shown was obtained by using the aforementioned translation and rotation panels. The other planets and spacecraft are not shown because of the 'closeness' of the view of the inner heliosphere.

As can be seen by examining the spiral colors in Figure 5, the flux intensities are decreasing with increasing planetary distance except for the case of Venus. More precisely, the flux at Venus is greater than that at Mercury for these particles. Consultation of the solar system graph immediately justifies this seeming contradiction as it shows that the footpoint of the Archimedean spiral path going from the sun to Venus is in the vicinity of the flare, whereas the footpoint of the Mercury spiral is not.
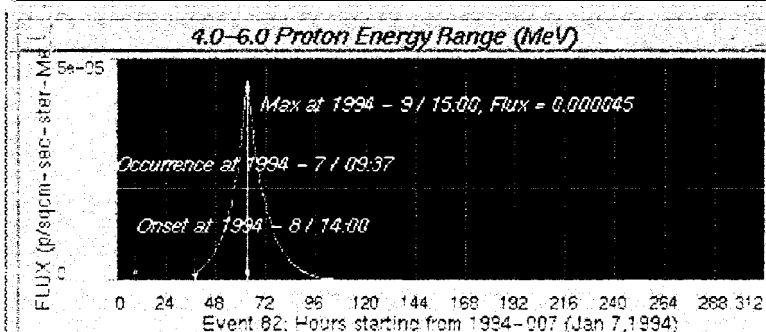
Graphical User Interface!

To yield further flux information regarding any of the planets or spacecraft shown in the solar system display panel of Figure 5, a graphical user interface was developed. A subset of the components of this interface is shown in Figure 6. In the lower right hand panel, we see a listing of events, planets and spacecraft similar to that shown in Figure 5 except that here there is a listing of proton

---

9. For each point τ, the graph used is that which represents the flux of protons at τ which have energy > 30 MeV. Other Energy range options are available. This was chosen as the measurement of flux intensities > 30 MeV are useful in determining the effects of protons upon spacecraft equipment.

0.8–1.2 Proton Energy Range (MeV)

FLUX (p/sqcm-sec-ster-MeV)

Max at 1994 – 9 / 16:00, Flux = 0.136011

Occurrence at 1994 – 7 / 09:37

Onset at 1994 – 8 / 15:00

0.2

0.1

0

0 24 48 72 96 120 144 168 192 216 240 264 288 312
Event 82: Hours starting from 1994–007 (Jan 7,1994)

| Help | Log | Linear | save | Dismiss |

Group Proton Energy Range (MeV)

FLUX (p/sqcm-sec-ster-MeV)

2e-06

1e-06

0

0 24 48 72 96 120 144 168 192 216 240 264 288 312
Event 82: Hours starting from 1994–007 (Jan 7,1994)

MeV Ranges
8.0–16.0
16.0–215.0
9.0–11.0
49.0–51.0
> 50.0

| Help | Log | Linear | Save | Dismiss |

VULCAN (Visual Utility for the Localization of Corona Accelerated Nuclei)

4.0–6.0 Proton Energy Range (MeV)

FLUX (p/sqcm-sec-ster-M

Max at 1994 – 9 / 15:00, Flux = 0.000045

Occurrence at 1994 – 7 / 09:37

Onset at 1994 – 8 / 14:00

5e-05

0

0 24 48 72 96 120 144 168 192 216 240 264 288 312
Event 82: Hours starting from 1994–007 (Jan 7,1994)

| Help | Log | Linear | Save | Dismiss |

VULCAN Help

Help Information

Message Windows

Flare Events

```
80  1994  Jan   5  16:56  [lat:2,   lon:-47]
81  1994  Jan   5  17:54  [lat:-10,  lon:24]
82  1994  Jan   7  09:37  [lat:-9,   lon:45]
83  1994  Jan   7  12:31  [lat:-4,   lon:44]
84  1994  Jan   9  22:44  [lat:-6,   lon:76]
```

System Messages

```
Mon 02/27/95 14:24:44 Event 80: No channel has proton fluxes abo
Mon 02/27/95 14:24:49 Event 78: No channel has proton fluxes abo
```
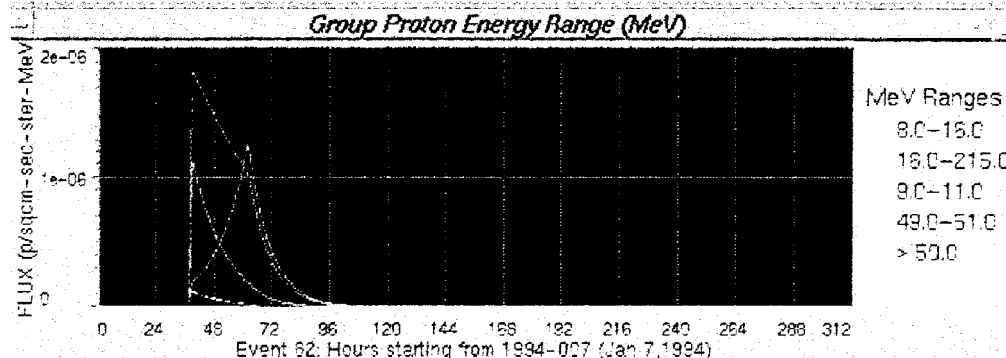
VULCAN – Visual Utility for the Localization
of" Corona Accelerated Nuclei

DEVELOPERS

Task Manager: Ursula   Schwuttke
Integration/Graphics: ,   Cecil   ia   Han
Graphical User Interface: ,, Felipe Hervias
Mathematical   Algorithms: J. Spagnuolo Jr.

problems, bug reports-, or suggestions, please contact

Comparisons

Inner Heliospheric Planets

| ^ Events | ∨ Planets | ∨ Mercury | ^ Venus [Magellan] | ∨ Earth [Topex] | ∨ Mars |

Proton Energy Range Selection (MeV)

1.0–4.0	16.0–215.0	9.0–11.0	> 10.0	>100.0	– 1	‹none›
4.0–8.0		14.0–16.0	> 30.0	> 500.0	‹none›
8.0–16.0	4.0–6.0	49.0–51.0	> 50.0	‹none›	‹none›

Flux Plotting (for selected ranges)

| Help | Query | Threshold | Single | Group | Quit |

| Dismiss |

energy ranges in megavolts. The user obtains this energy panel by clicking the energy range button in the flare events window as shown in Figure 5. Suppose that the user wishes to find out exact flux values in the vacinity of Venus. He first selects the flare event of interest (#82 for purposes of illustration and then activates the Venus button. To see an overlay of flux graphs for various energy ranges at Venus, the user first clicks on the button corresponding to each range of interest and then clicks on the Group button occurring at the bottom of the energy window. A set of graphs then appears as displayed in the window directly above the flare events window. The graphs are color coded, with the keys appearing at the right hand side of the display. If the user selects the Single button then a set of windows will appear, one for each energy range selected. In each window, a single flux graph will appear corresponding to a preselected energy range. For convenience we illustrate only two of these diagrams, one for protons falling in the 0.8 to 1.2 megavolt range and one for protons in the 4.0 to 6.0 energy range. For each energy range, we list the onset time' the time of flare occurrence (UTM) anti the time and value of maximum flux. Since the user chose the Venus button, the onset times and time of maximum flux are for Venus. For each window, log plots are available. The user also has the option of saving the diagram to a file for easy access.

Figure 7 gives a complete view of the solar wind. In the actual program, the correct motion of the spirals as they extend to the inner heliosphere is modeled. The r-sun plane as described earlier is also displayed.

Summary

We have developed a system which receives data in real time from Boulder Colorado and uses ephemeris data to predict the effects of solar flares on the planets and spacecraft of the inner heliosphere. Further, the system allows the individual to enter events of his own construction or those on record to determine what fluxes will result be they in the past or future. Graphical user interfaces

10. Time at which the protons reach the point of interest.

VULCAN (Visual Utility for the Localization of Corona Accelerated Nuclei)

File Demos Grids Options

Translation   Rotation   Hour   12
X   X   313
Y   Y   Day
Z   Z   Year   1990

☐ Insignificant
☐ Significant Threshold >   12
☐ Serious Threshold >   20
■ Critical Threshold >   50

Mars
X
Galileo
Earth

Z

Sun
Jupiter

Mercury

Venus   Saturn
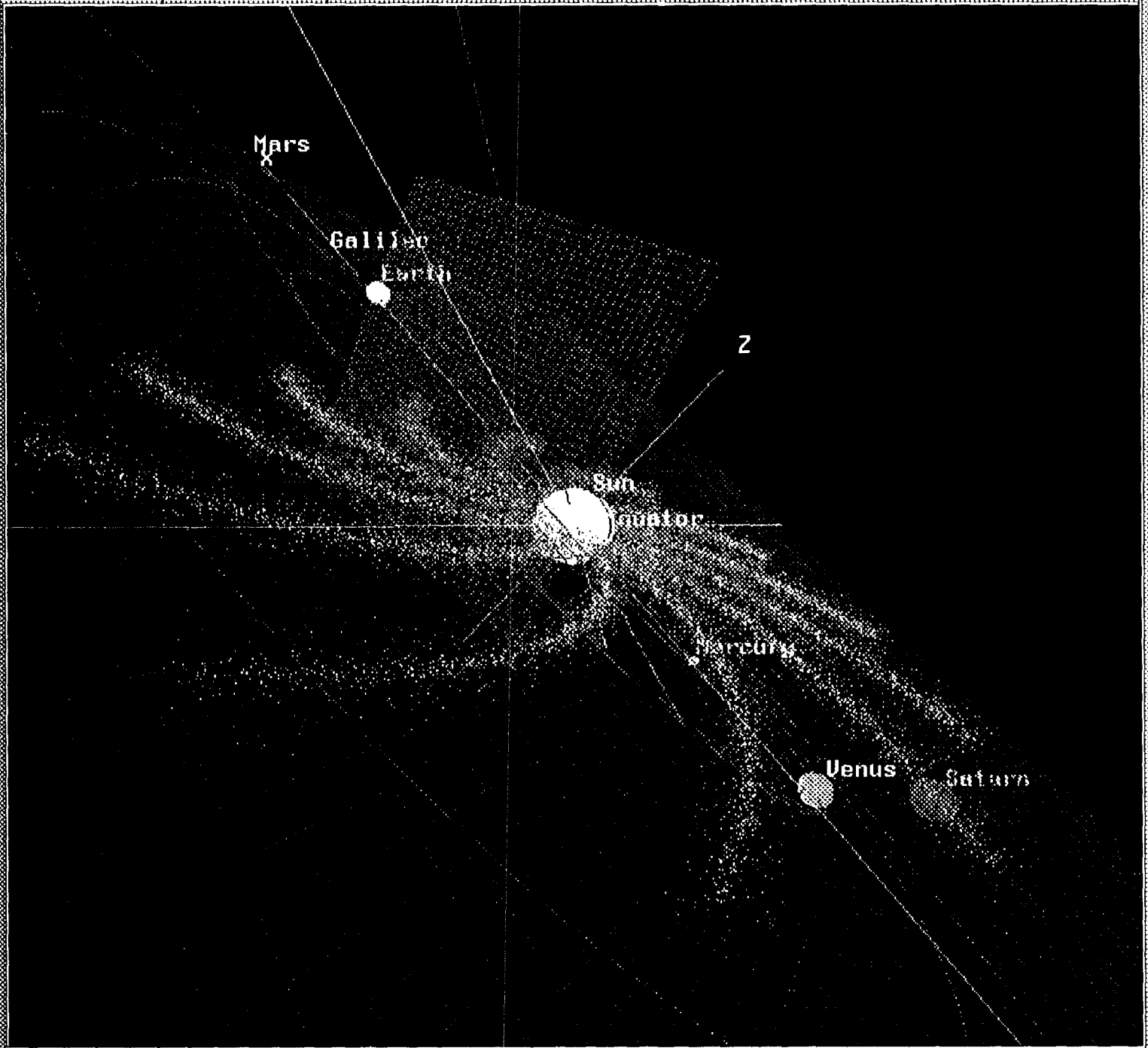
together with manipulable views of the solar system and color coding of proton flux paths facilitate experimentation with various parameters to determine how an alteration of their values influence variations on the distribution of solar particles at points in or near the solar system.

References

[1] Robinson, P.A.Jr., "The Effects of High Energy Particles on Planetary Missions," *Proceedings of the JPL Workshop in the Interplanetary Charged Particle Environment*, edited by J. Feynman and S.Gabriel, NASA JPL Publication 88-28, April 15, 1988, pp.39-46.

[2] Spitale, G.C., "Solar Event Environment at Mars at the Time of Loss of Communications with Mars Observer," JPL Interoffice Memorandum 5215-93-267, Pasadena California, October 5, 1993.

[3] Richter, R., Spagnuolo, J. Jr.,"Energetic Solar Particle Activity during the Time of Astral-B Failure," JPL Interoffice Memorandum 3544-TOP-94-001, Pasadena California, January 3, 1994.

[4] Smart,D.F., Shea,M.A.," PPS76 - A computerized "event mode" solar proton forecasting technique," *Solar Terrestrial Prediction Proceedings*, edited by R.F. Donnelly, Vol.1, U.S Department of Commerce, NOAA/ERL, 1979, pp.406-423.

[5] Smart,D.F., Shea,M,A.," Galactic cosmic radiation and solar energetic particles," Chapter 6 in *The Handbook of Geophysics and the Space Environment*,edited by A. S. Jursa, Airforce Geophysics Laboratory, Bedford, Massachussetts,1985,Chapter 6.

[6] Heckman, G.R., Kunches, J.M., Allen, J.H., "Prediction and evaluation of solar particle events based on precursor information", Advances in Space Research, Vol 12, No. 2-3 , 1992, pp2(313)-2(320

[7] Cliver, E.W., Secan, J.A., Bea d, E.D., Manley, J.A., " Prediction of Solar Proton Events at the Air Force Global Weather Central's Space Environmental Forecasting Facility," *Proceedings of the 1978 Symposium on the Effect of Ionosphere on Space and Terrestrial Systems*, Arlington, Va, 1978, pp.393-400.

[8] Acton, C.H. Jr., "Using the Spice System to Help Plan and Interpret Space Science Observations", Proceedings of SPACEOPS 92: The Second International Symposium on Ground Data Systems for Mission Operations, paper # K.4, March 1, 1993.

[9] Smart, D.F., Shea, M.A., "Predicting and Modeling Solar Flare Generated Proton Fluxes in the Inner Heliosphere", Space Physics Division, Geophysics Directorate, Phillips Laboratory, 1992.

[10] Smart, D.F., Shea, M.A., "Modeling the Time Intensity Profile of Solar Flare Generated Particle Fluxes in the Inner Heliosphere", Advances in Space Research, Vol 12, No. 2-3 , 1992, pp2(303)-2(312).

[11] Parker, E.N., "Interplanetary Dynamical Processes", Monographs and Texts in Physics and Astronomy, edited by R.E.Marshak, Vol 8, Interscience Publishers, New York, 1963.